Geophysical Research Letters

RESEARCH LETTER
10.1029/2020GL088476

Mid-Holocene Grounding Line Retreat and Readvance at Whillans Ice Stream, West Antarctica

R. A. Venturelli[1], M. R. Siegfried[2,3], K. A. Roush[4], W. Li[4], J. Burnett[5], R. Zook[6], H. A. Fricker[3], J. C. Priscu[4], A. Leventer[7], and B. E. Rosenheim[1]

[1]College of Marine Science, University of South Florida, St. Petersburg, FL, USA, [2]Department of Geophysics, Colorado School of Mines, Golden, CO, USA, [3]Institute of Geophysics and Planetary Physics, Scripps Institution of Oceanography, University of California, San Diego, La Jolla, CA, USA, [4]Department of Land Resources and Environmental Science, Montana State University, Bozeman, MT, USA, [5]Applied Physics Laboratory, University of Washington, Seattle, WA, USA, [6]University of Nebraska–Lincoln, Lincoln, NE, USA, [7]Department of Geology, Colgate University, Hamilton, NY, USA

Key Points:
- Direct evidence is found for mid-Holocene grounding line retreat on the Siple Coast, West Antarctica
- Chronological constraints at Whillans Ice Stream imply western Ross Sea forcing on the southern Siple Coast, in contrast to other Siple Coast ice streams
- Ramped PyrOx allows for accurate ^{14}C dating of low carbon, grounding-line-proximal sediments

Supporting Information:
- Supporting Information S1
- Table S1
- Movie S1

Correspondence to:
R. A. Venturelli,
raventurelli@mail.usf.edu

Citation:
Venturelli, R. A., Siegfried, M. R., Roush, K. A., Li, W., Burnett, J., Zook, R., et al. (2020). Mid-Holocene grounding line retreat and readvance at Whillans Ice Stream, West Antarctica. *Geophysical Research Letters*, *47*, e2020GL088476. https://doi.org/10.1029/2020GL088476

Received 24 APR 2020
Accepted 13 JUL 2020
Accepted article online 19 JUL 2020
Corrected 24 OCT 2020

This article was corrected on 24 OCT 2020. See the end of the full text for details.

Abstract Understanding ice sheet evolution through the geologic past can help constrain ice sheet models that predict future ice dynamics. Existing geological records of grounding line retreat in the Ross Sea, Antarctica, have been confined to ice-free and terrestrial archives, which reflect dynamics from periods of more extensive ice cover. Therefore, our perspective of grounding line retreat since the Last Glacial Maximum remains incomplete. Sediments beneath Ross Ice Shelf and grounded ice offer complementary insight into the southernmost extent of grounding line retreat, yielding a more complete view of ice dynamics during deglaciation. Here we thermochemically separate the youngest organic carbon to estimate ages from sediments extracted near the Whillans Ice Stream grounding line to provide direct evidence for grounding line retreat in that region as recent as the mid-Holocene (7.2 kyr B.P.). Our study demonstrates the utility of accurately dated, grounding-line-proximal sediment deposits for reconstructing past interactions between marine and subglacial environments.

Plain Language Summary Ice sheet grounding lines, where ice loses contact with the underlying bed and transitions to an ice shelf floating on the ocean, are critical areas that govern the stability of marine-based ice sheets. However, the short period (years to decades) that we have been able to map grounding lines from ground, airborne, and satellite observations compared to the long periods over which ice sheets change (centuries to millenia) limits our knowledge of grounding line stability. We focus our geologic perspective of grounding line retreat in the Ross Sea, a region that has experienced a high degree of change throughout the last glacial-interglacial cycle. Prior work reconstructing the timeline of ice sheet change in this region is based heavily on ice-free marine sedimentary records, where dates of the first open marine sedimentation after ice retreat can be estimated. Dating sediments from beneath floating ice shelves and near grounding lines has proven difficult for both logistical and methodological reasons, limiting our understanding of grounding line evolution. We used novel radiocarbon dating methods on sediments collected from beneath the floating Ross Ice Shelf to find that the grounding line retreated inland of the current position during the mid-Holocene and subsequently readvanced.

1. Introduction

The West Antarctic Ice Sheet (WAIS) is a marine-based ice sheet susceptible to rapid retreat and possible collapse in the face of projected warming (e.g., DeConto & Pollard, 2016; Golledge et al., 2015; Mercer, 1978). The marine ice sheet instability (MISI) hypothesis suggests that ice sheet grounding lines, where ice transitions from grounded to floating, are critical for large-scale ice sheet evolution (e.g., Hughes, 1973; Mercer, 1978; Schoof, 2007; Weertman, 1974). Through both observations and modeling, it has been demonstrated that multiple processes can individually or cumulatively impact the stability of a grounding line on different timescales: sea level (e.g., Schoof, 2007); intrusion of warm water (Rignot & Jacobs, 2002), isostatic adjustment (e.g., Gomez et al., 2010; Whitehouse et al., 2019); underlying topography and bathymetry (e.g., Halberstadt et al., 2016; Matsuoka et al., 2015); and sedimentary accumulation (e.g., Alley et al., 2007; Simkins et al., 2018). Therefore, quantifying long-term stability of WAIS grounding lines can constrain estimates of future contributions of Antarctic Ice Sheet mass loss (DeConto & Pollard, 2016). Despite the long

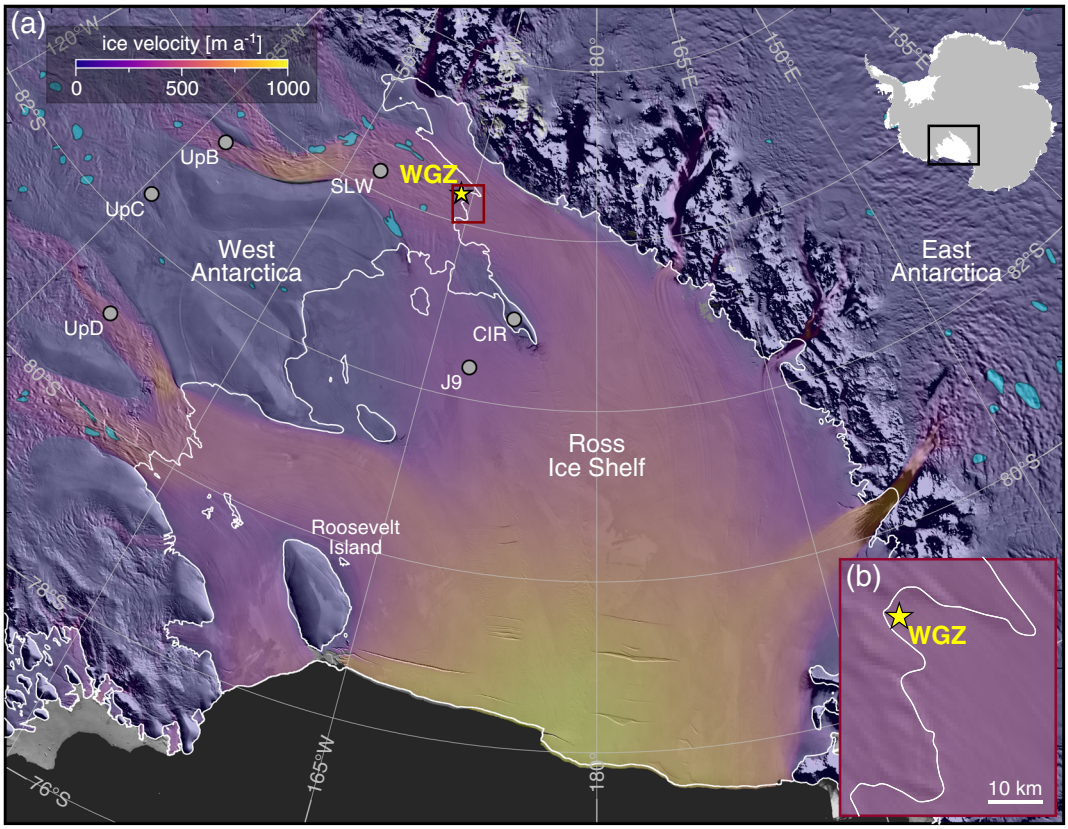

Figure 1. Map of study location. (a) Ross Sea sector (inset showing extent on Antarctica) with historical subglacial core site locations (gray circles) and Whillans Grounding Zone (WGZ) site (this study; yellow star). Ice velocity (Mouginot et al., 2019) overlain on an imagery mosaic (Scambos et al., 2007), with active subglacial lake areas (blue polygons; Siegfried & Fricker, 2018) and grounding line (white; Depoorter et al., 2013) indicated. (b) WGZ embayment showing core site relative to grounding line.

timescales over which grounding line dynamics can change, direct observations of grounding line dynamics have only been made over the past decade (e.g., Joughin et al., 2016; Rignot et al., 2014). Present-day sub-ice sediments provide an underexplored archive of grounding line retreat and advance, which can be leveraged to extend the record of grounding line stability into the geologic past.

Deglaciation of the Ross Sea since the Last Glacial Maximum (LGM) provides one of the best examples of significant Antarctic ice retreat in the geologic record and thus serves as an analog for the future of marine-based ice sheet sectors. Marine geological evidence on the Ross Sea continental shelf (e.g., Anderson et al., 2002, 2014; Bentley et al., 2014; Mosola & Anderson, 2006; Simkins et al., 2018) and terrestrial evidence surrounding the Ross Sea (e.g., Hall & Denton, 2000; Hall et al., 2013; Spector et al., 2017; Stuiver et al., 1981) have been used to chronicle the pattern of retreat during the last deglaciation. Although this region has been heavily investigated, there remains an active debate surrounding the style and timing of deglaciation here. The paradigm of a "swinging gate" deglacial pattern persisted for several decades, wherein Roosevelt Island serves as a pinning point in the eastern Ross Sea, and the grounding line migrates southward along the Transantarctic Mountains in the western Ross Sea (Conway et al., 1999). More recently, periods of rapid Holocene retreat (Spector et al., 2017) and readvance (Greenwood et al., 2018; Kingslake et al., 2018) have been suggested, and varied styles of retreat resulting from differences in physiography and bathymetry across the Ross Sea have been proposed (Halberstadt et al., 2016; Prothro et al., 2020).

Evaluating the full extent of deglaciation in the Ross Embayment requires dateable deposits from beneath the contemporary Ross Ice Shelf (RIS); however, thick ice cover, with 95% of RIS area between 211 and 764 m thick (Morlighem, 2019; Morlighem et al., 2020), limits direct access to these sediments. Before the

Whillans Ice Stream Subglacial Access Research Drilling (WISSARD) Project, the only sediment samples retrieved from beneath RIS were collected at site J9 (Figure 1a) as part of the RIS Project (Clough & Hansen, 1979). Sediments from J9, along with sediments from beneath the Siple Coast ice streams flowing into RIS (Figure 1a), contain Miocene, Pliocene, and Pleistocene aged microfossils (Coenen et al., 2019; Harwood et al., 1989; Scherer, 1991, Scherer et al., 1998), as well as measurable radiocarbon (Kingslake et al., 2018). Knowledge that diachronous marine influence on subglacial sediments introduces a chronologic range on the order of millions of years should thus raise caution on how time-diagnostic data from subglacial sediments are interpreted. We analyzed a grounding-line-proximal sediment core from Whillans Ice Stream to provide accurate chronological constraints on grounding line stabilization. We employed Ramped PyrOx (RPO) radiocarbon (^{14}C) dating, specifically designed to thermochemically deconvolve mixtures of acid-insoluble organic material (AIOM) and remove biases from glacially reworked carbon, to directly test a recent model-based hypothesis of Holocene grounding line retreat and readvance (Kingslake et al., 2018).

2. Study Location and Methods

2.1. Study Location and Borehole Operations

The Whillans Ice Stream grounding zone (WGZ) is one of the most studied areas of WAIS (e.g., Christianson et al., 2013; Horgan, Alley, et al., 2013; Horgan, Christianson, et al., 2013; Jacobel et al., 2014; MacGregor et al., 2011). WGZ is influenced by glacial and glaciofluvial processes, including sediment transport downstream by till deformation (e.g., Alley et al., 1986; Blankenship et al., 1986; Kamb, 2001), englacial sediment transport and deposition by basal melt (e.g., Christianson et al., 2016; Christoffersen et al., 2010), and transport of suspended sediment by the subglacial hydrologic system (e.g., Alley, 1989; Horgan, Christianson, et al., 2013). Though an actively accreting grounding zone wedge has been identified elsewhere in the Whillans Ice Stream system (Alley et al., 2007; Anandakrishnan et al., 2007), a comprehensive geophysical survey across the grounding line at our study site (84.33543°S, 163.61187°W; Figure 1b) identified no evidence for grounding zone wedge deposition (Horgan, Christianson, et al., 2013). Instead, the sedimentary system accessed as part of the WISSARD Project (2014–2015) consists of recent sedimentation from basal melt (Movie S1 in the supporting information) underlain by subglacial till (Horgan, Christianson, et al., 2013). We collected a 70 cm-long gravity core through a hot-water-drilled borehole (Rack, 2016; Tulaczyk et al., 2014) located ~3 km downstream from the modern grounding line of Whillans Ice Stream (Begeman et al., 2018, 2020).

2.2. Geochemical and Microfossil Preparation

We determined total organic carbon (%TOC) of WGZ sediments (Text S1) with a Carlo-Erba NAN2500 Series-II Elemental Analyzer using a small aliquot of each sample. We prepared individual samples (5, 13, 40, and 62 cm) for radiocarbon dating with RPO, which employs a temperature ramp of 5°C per minute to leverage the thermochemical reactivity of AIOM within a sediment sample (Rosenheim et al., 2008; Text S2). Aliquots of CO_2 from RPO preparation were sent to the National Ocean Sciences Accelerator Mass Spectrometry (NOSAMS) facility for determination of $^{14}C/^{12}C$ ratios and $\delta^{13}C$. We prepared slides for individual samples (3, 32, and 64 cm) after the methods of Scherer (1994) and Warnock and Scherer (2015), which allows for a random distribution of diatoms to be settled over a known surface area for quantification of absolute diatom abundance.

2.3. RPO Data Treatment

We normalized the thermograph (evolution of CO_2 as a function of temperature from the RPO process) of each sample to total pCO_2 produced in each run to compare the thermochemical stability of carbon separation at each core depth. We iteratively decomposed each thermograph into reaction components, assuming a Gaussian distribution of activation energies in the temperature domain within each component and using a nonlinear least squares technique to minimize residuals. To quantitatively relate information from thermographs to carbon bond strength and chemical stability, we modeled thermal activation energy distributions for each sample following Hemingway (2017) and Hemingway et al. (2017). We blank corrected all ^{14}C ages to account for uncertainty due to the RPO preparation process (Fernandez et al., 2014; Text S3). We calibrated radiocarbon ages (^{14}C year) of low temperature RPO intervals to calendar years (year B.P.) using the Marine20 curve in Calib 8.2 (Heaton et al., 2020) and a local reservoir correction of 1,101 ± 120 years

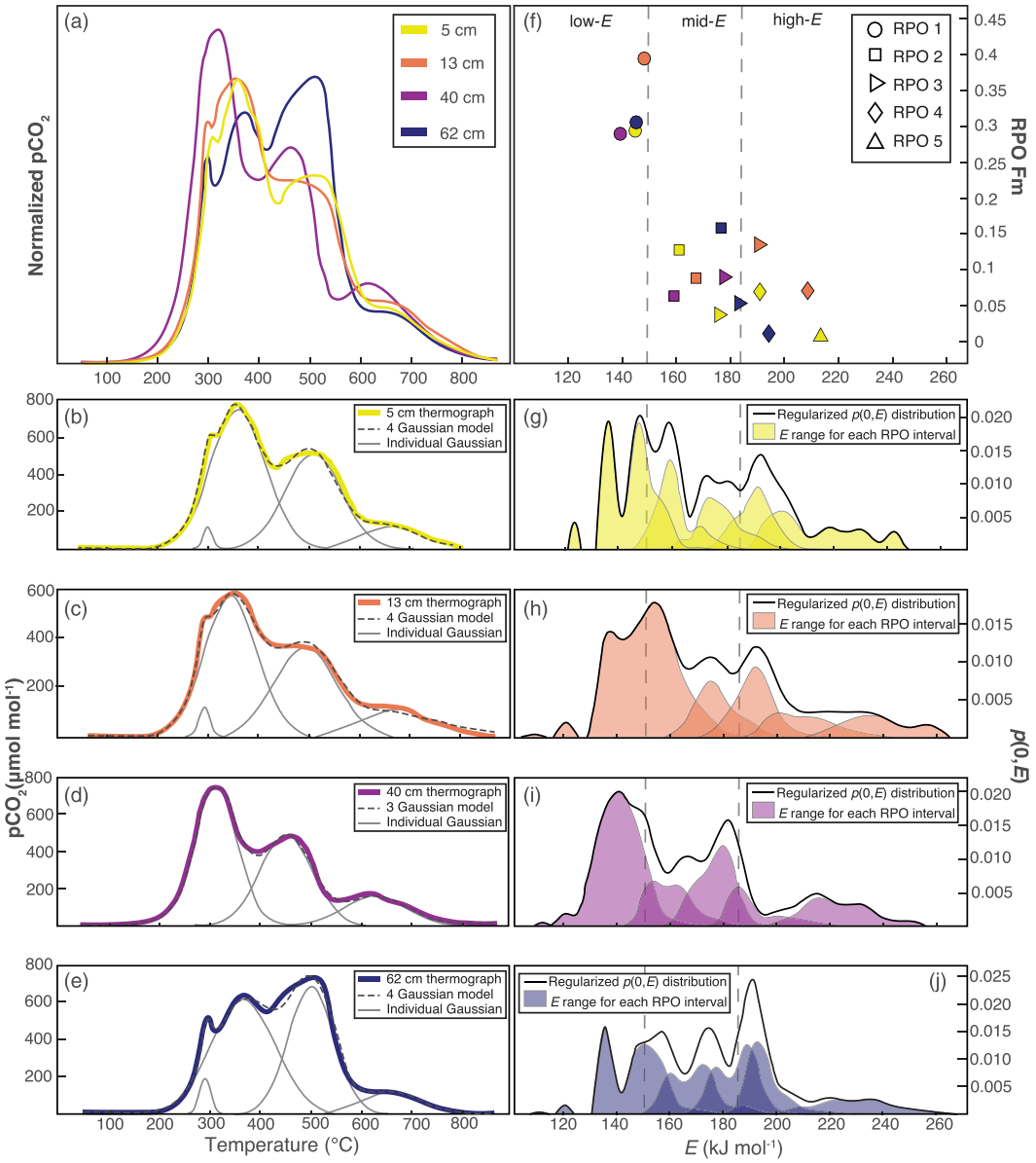

Figure 2. (a) Thermographs for all samples. Gaussian decompositions of thermographs for (b) 5, (c) 13, (d) 40, and (e) 62 cm core depths, showing modeled temperature ranges for individual carbon components. (f) Activation energy (E) versus fraction modern (Fm) for all RPO intervals with measurable ^{14}C activity. Dotted lines separate organic carbon into low-E (<150 kJ mol^{-1}), mid-E (150–185 kJ mol^{-1}), and high-E (>185 kJ mol^{-1}). Modeled energy distributions ($p(0, E)$) at (g) 5, (h) 13, (i) 40, and (j) 62 cm core depths show the range of energy distributions in each RPO interval.

reflecting measured living amphipods from the site and prescribed uncertainties on reservoir ages due to different water masses intruding onto the Antarctic margin (Hall et al., 2010; King et al., 2018; Kingslake et al., 2018; Text S4).

3. Results

3.1. Thermographs and Activation Energy Distributions

Separation of AIOM with RPO results in qualitative information about thermochemical stability (Figures 2a–2e) and quantitative information about the stability of organic carbon in these sediments (Figures 2f–2j). Samples analyzed at 5, 13, and 62 cm fit a four-component Gaussian model (Figures 2b,

Table 1
Table of Radiocarbon Results

Sample	Sample size (μmol)	Reported Fm	± (1σ)	Blank corrected Fm	± (1σ)	Age (^{14}C years)	± (1σ)	δ^{13}C (‰)
WGZ 5 cm: RPO 1	12.4	0.3046	0.0012	0.2952	0.0080	9,800	220	−27.6
WGZ 5 cm: RPO 2	19.1	0.1375	0.0012	0.1287	0.0064	16,450	300	−25.7
WGZ 5 cm: RPO 3	14.8	0.1031	0.0011	0.0910	0.0084	19,250	740	−25.7
WGZ 5 cm: RPO 4	12.5	0.0852	0.0012	0.0705	0.0101	21,300	1,200	−25.1
WGZ 5 cm: RPO 5	24.2	0.0158	0.0011	0.0073	0.0057	39,500	6,300	−22.2
WGZ 13 cm: RPO 1	12.1	0.4032	0.0013	0.3961	0.0073	7,440	150	−30.3
WGZ 13 cm: RPO 2	13.5	0.1703	0.0010	0.1586	0.0085	14,800	430	−27.3
WGZ 13 cm: RPO 3	12.7	0.1492	0.0010	0.1363	0.0093	16,000	550	−27.1
WGZ 13 cm: RPO 4	12.4	0.0869	0.0009	0.0721	0.0102	21,100	1,100	−27.6
WGZ 13 cm: RPO 5	10.3	0.0170	0.0009	−0.0030	0.0132	*>30,200*	—	−22.9
WGZ 40 cm: RPO 1	13.4	0.2992	0.0137	0.2904	0.0158	9,930	440	−29.0
WGZ 40 cm: RPO 2	15.2	0.0771	0.0008	0.0648	0.0084	22,000	1,000	−26.8
WGZ 40 cm: RPO 3	15.4	0.0510	0.0008	0.0383	0.0085	26,200	1800	−26.1
WGZ 40 cm: RPO 4	13.6	0.0128	0.0008	−0.0024	0.0100	*>32,400*	—	−26.4
WGZ 40 cm: RPO 5	11.8	0.0122	0.0008	−0.0053	0.0116	*>32,400*	—	−21.2
WGZ 62 cm: RPO 1	13.6	0.3154	0.0012	0.3070	0.0073	9,490	190	−28.3
WGZ 62 cm: RPO 2	16.6	0.1005	0.0011	0.0897	0.0075	19,350	680	−27.2
WGZ 62 cm: RPO 3	17.5	0.0649	0.0011	0.0540	0.0074	23,400	1,100	−26.5
WGZ 62 cm: RPO 4	24.1	0.0199	0.0011	0.0114	0.0057	35,900	4,000	−25.6
WGZ 62 cm: RPO 5	16.6	0.0087	0.0012	−0.0038	0.0083	*>35,000*	—	−21.0

Note. Reported fraction modern (Fm) is data directly from NOSAMS. Blank Corrected Fm values have been corrected to account for uncertainty resulting from RPO preparation. Italicized items are used to show that these ages are near the limits of measurable radiocarbon.

2c, and 2e), whereas the 40 cm sample did not contain the low temperature Gaussian component present at other depths, fitting best with a three-component Gaussian model (Figure 2d). The 5, 13, and 40 cm samples reacted at lower temperatures, represented by a large low temperature (350°C) peak, whereas the 62 cm eluted more CO_2 at a higher temperature (505°C). Thermal decomposition activation energy distributions (Figures 2g–2j) reveal that RPO intervals range in activation energies across low (<150 kJ mol^{-1}), medium (150 $\leq E <$ 185 kJ mol^{-1}), and high (≥185 kJ mol^{-1}) energy ranges, demonstrating that subglacial organic carbon contains diverse bond structures rather than a homogeneous pool of refractory carbon (Hemingway et al., 2018). We separated the low-energy component in the lowest temperature interval of each of our samples, which yielded distinctly different activation energies from higher temperature intervals (Figure 2f). Though not useful for chronological purposes, higher temperature RPO intervals (RPO 2–5) were characterized by higher activation energies. Generally, these fractions contain less radiocarbon (i.e., are older) than other fractions (Rosenheim & Galy, 2012; Rosenheim, Roe, et al., 2013; Rosenheim, Santoro, et al., 2013; Williams et al., 2015), unless the low-energy radiocarbon from was from a frozen labile source like permafrost (Schreiner et al., 2014; Zhang et al., 2017) or volatile petroleum carbon (Pendergraft & Rosenheim, 2014). Combined with stable isotopic data, mid- and high-*E* data can be useful in Antarctic sediments for identifying sources and amounts of relict organic carbon in a grounding-line-proximal environment.

3.2. Geochemical and Diatom Data

Sediments from WGZ had low %TOC (0.03–0.21%; Table S1) and low diatom abundances (500 to 1,000 valves per gram dry sediment; Text S5). The most commonly observed diatom species were *Denticulopsis simonsenii*, *Pyxilla reticulata*, *Stephanopyxis* sp., and *Paralia sulcata*. None of the diatom specimens observed in our study were species that are common living taxa in the modern Ross Sea. Five aliquots of CO_2 at 5, 13, 40, and 62 cm resulted in a spectrum of isotopic data and ^{14}C ages for all samples (Table 1; Figure 3). The most thermochemically reactive aliquot of carbon was separated into the lowest-temperature RPO interval, containing 15% of the total sample at 5, 40, and 62 cm and 19% of the total sample at 13 cm determined by mass. Low-temperature aliquots for each sample contained the highest ^{14}C concentrations for each of the four spectra, resulting in ages from 9,900 to 7,400 ^{14}C year and lacking stratigraphic order (Figure 3). Values of δ^{13}C ranged from −30.3% to −27.6‰ VPDB in low temperature intervals. Radiocarbon concentrations decreased throughout the spectra, resulting in increasing ages and increasing δ^{13}C values with

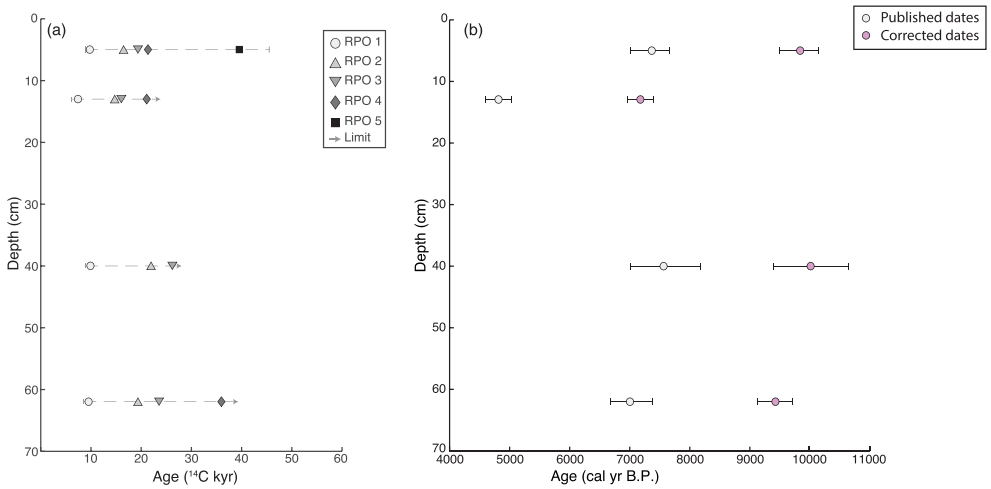

Figure 3. (a) RPO ^{14}C age spectra and (b) calibrated radiocarbon ages for low temperature RPO intervals. Where intervals are not indicated with a point in (a), radiocarbon content was less than the uncertainty of radiocarbon content or negative. We display these intervals with an arrow toward higher age to indicate limitations of reporting radiocarbon concentrations close to background.

temperature (Table 1). High temperature intervals from 13, 40, and 62 cm samples resulted in ^{14}C sample activity less than the uncertainty of radiocarbon content and are reported as minimum ages after Stuiver and Polach (1977). Weighted arithmetic means of age spectra result in ages of 26,800–14,900 ^{14}C years, not in stratigraphic order (Table S1).

4. Discussion

4.1. RPO Under Ice

The WGZ sedimentary system is composed of material influenced by glacial and subglaciofluvial processes (e.g., Christianson et al., 2013; Horgan, Alley, et al., 2013; Horgan, Christianson, et al., 2013; Vick-Majors et al., 2020). In a sub-ice shelf setting, the proportion of preaged carbon transported from the continent (allochthonous material) is present in much higher proportion than carbon input from the marine environment (autochthonous material), with ages of these components reflecting the dynamic processes occurring before deposition (Subt et al., 2017). The application of RPO at WGZ builds upon previous work with Antarctic marine sediments to improve deglacial chronology by exploiting differences in thermochemical stability between autochthonous organic material and allochthonous organic material (Rosenheim et al., 2008; Rosenheim, Roe, et al., 2013; Subt et al., 2016, 2017). In order to interpret ^{14}C concentrations measured in low-carbon, subglacial sediments as a chronological constraint on grounding line retreat, separation of autochthonous organic material from high proportions of allochthonous material is imperative.

4.2. Comparison to Previous ^{14}C Dating

We identify the presence of 9,900 to 7,400 ^{14}C year old (Figure 3a) organic carbon in low temperature RPO intervals throughout our core. Recent work interpreted the presence of radiocarbon from bulk-dated subglacial sediment samples at WGZ, as well as upstream Whillans, Kamb, and Bindschadler ice streams, as evidence for exposure of the subglacial environment to marine water during the Holocene (Kingslake et al., 2018). This interpretation is consistent with stable carbon isotopic data in our study, falling within a typical range of marine organic material in the Ross Sea (Villinski et al., 2000). The lack of common modern Ross Sea diatoms observed here implies that marine incursion occurred under sub-ice-shelf conditions rather than with the onset of open marine conditions (Smith et al., 2019). Dissolved inorganic carbon beneath RIS can be fixed by chemolithoautotrophic ammonium oxidizing bacteria to produce new particulate organic carbon (Horrigan, 1981; Priscu et al., 1990). Therefore, the presence of radiocarbon in our

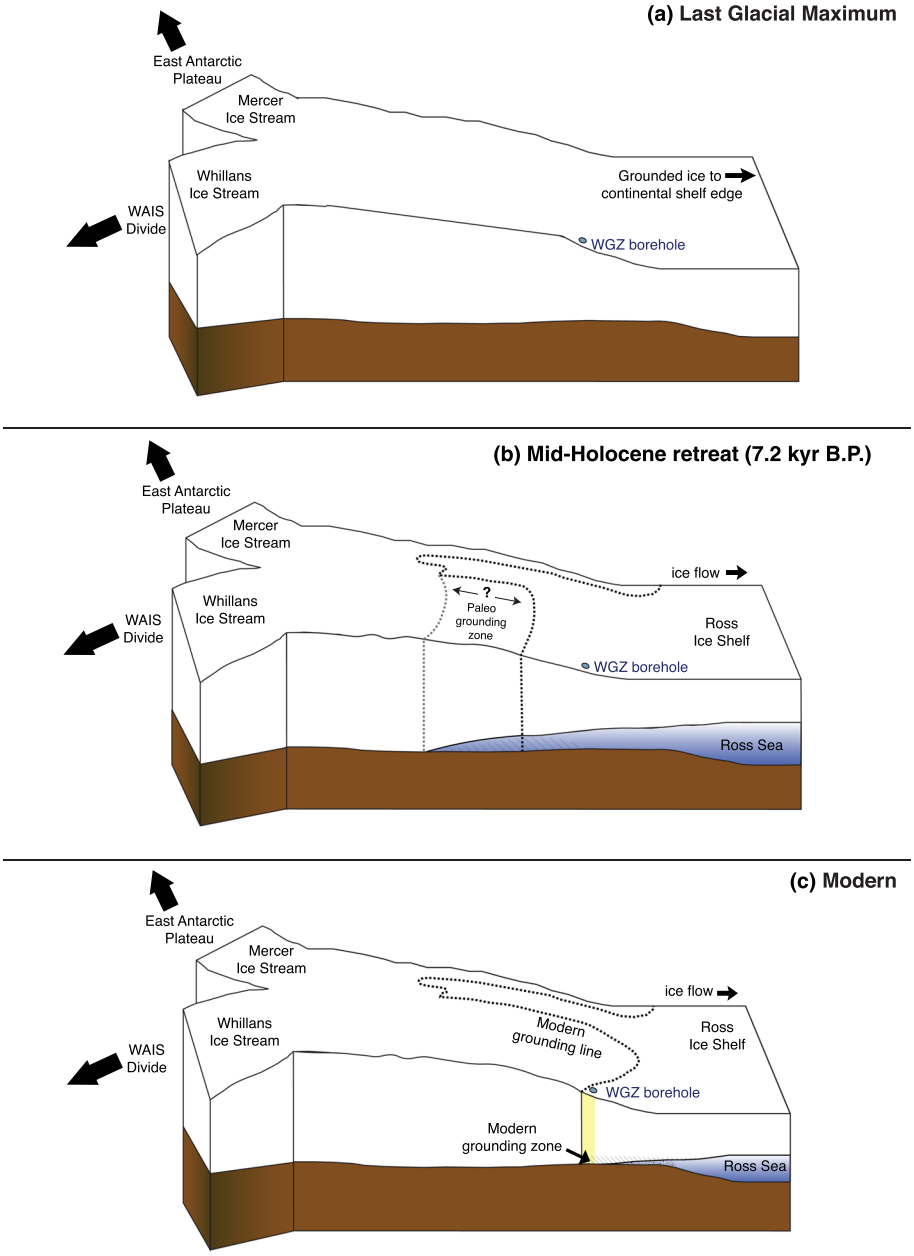

Figure 4. Conceptual model illustrating Whillans Ice Stream grounding zone line through (a) LGM, (b) Mid-Holocene retreat (7.2 kyr B.P.), and (c) readvance to present position (Depoorter et al., 2013) based on RPO ^{14}C ages in this study.

sediments likely reflects the timing of this microbial process when the subglacial environment was exposed to marine water.

Weighted arithmetic means of RPO age spectra are comparable to bulk-dated ages from the same AIOM samples taken from riverine settings (Rosenheim & Galy, 2012) and the Bellingshausen Sea (Rosenheim, Roe, et al., 2013); in highly detrital sediments, however, weighted arithmetic mean ages have been shown to result in slightly younger ages than conventional bulk dates (Subt et al., 2017). Bulk-dated samples from other WGZ cores resulted in ages from 28,600 to 20,200 ^{14}C year (Kingslake et al., 2018). Mean ages calculated from RPO age spectra in our study resulted in ages ranging from 26,800 to 14,900 ^{14}C years old (Table S2). Younger calculated bulk ages for the same sediments may be explained by slight differences in pretreatment of material having a different effect on young labile organic carbon, as preparation techniques can influence dating efforts (Bao et al., 2019). Combined with heterogeneous sedimentation in a low-carbon,

ice-proximal depositional environment, small differences in extremely low ratios of $^{14}C/^{12}C$ can be expected when interpreted as ages, consistent with Subt et al. (2017). Nonetheless, low temperature RPO intervals here are 7,500 to 17,800 ^{14}C years younger than previously bulk-dated samples from WGZ (Kingslake et al., 2018).

4.3. Whillans Ice Stream Grounding Line Retreat

Isolation of low-energy bonded carbon in low-temperature RPO intervals demonstrates that we have minimized the amount of relict carbon incorporated in our dated samples, reducing geological uncertainty in dating grounding-line-proximal sediment. We calibrated our low temperature RPO intervals to calendar years (Figure 3b) and interpret the mid-Holocene ages (7.2 kyr B.P.) as chronological constraints of grounding line retreat. The incorporation of marine carbon in these sediments supports the hypothesis that the upstream Whillans Ice Stream subglacial system was previously exposed to the marine environment. These results imply that the grounding line retreated beyond its current position in the mid-Holocene and subsequently readvanced to the current position, rather than a progressive retreat of the grounding line in the Ross Sea since the LGM (Figure 4). Thus, the paradigm of a unidirectional retreat, pinned at Roosevelt Island at 3.2 kyr B.P. (e.g., Conway et al., 1999; Lowry et al., 2019), is not consistent with our results. WGZ RPO ^{14}C data support the model of grounding line and readvance following the LGM (Greenwood et al., 2018; Kingslake et al., 2018). However, our dates from WGZ indicate that grounding line retreat occurred at least 2 kyr later, during the mid-Holocene, rather than the early Holocene (9.7 kyr B.P.) as simulated by Kingslake et al. (2018).

4.4. Implications for Deglacial History of Ross Sea

Our record from WGZ provides new insight into the large-scale deglacial history of the Ross Sea. During the LGM, grounded ice filled the Ross Sea (Figure 4a) to the continental shelf edge (e.g., Bentley et al., 2014; Mosola & Anderson, 2006). Exposure ages indicate that Beardmore and Scott Glaciers, which deliver ice to the central Ross Sea, maintained LGM ice thickness until between 16.7 and 14.4 kyr B.P. (Spector et al., 2017). These terrestrial records are consistent with the marine AIO (Prothro et al., 2020) and foraminiferal (Licht, 2004) constrained ^{14}C ages for timing of initiation of grounding line retreat from the continental shelf edge. As deglaciation persisted in the western Ross Sea, foraminiferal ^{14}C ages indicate open marine conditions east of Ross Island 8.6 kyr B.P. (McKay et al., 2016), consistent with ^{10}Be exposure ages indicating grounding line retreat to the mouths of Beardmore and Shackleton glaciers (Spector et al., 2017). Collectively, these records indicate that full deglaciation of the western Ross Sea precedes grounding line retreat of Whillans Ice Stream by ~1 kyr. Dates from WGZ falls closer to the deglacial history in the western Ross Sea than in the eastern Ross Sea (e.g., Bart, Anderson, et al., 2017; Bart, Krogmeier, et al., 2017). This interpretation is consistent with the tectonic boundary identified between East and West Antarctica beneath RIS, which has been suggested to control bathymetry and oceanic circulation (Tinto et al., 2019). We thus contend that grounding line retreat at Whillans Ice Stream likely responded to western Ross Sea oceanic conditions, whereas grounding line retreat at other ice streams along the Siple Coast (i.e., Bindschadler ice stream) may have been more strongly influenced by eastern Ross Sea oceanic conditions. The occurrence of retreat at WGZ supports physiographic control of grounding line retreat through embayments (Halberstadt et al., 2016), but widespread transects of sub-ice sediment cores dated with RPO ^{14}C or similarly accurate methods are needed to fully constrain the southernmost extent of this process.

5. Conclusions

We present the most accurately dated record of sediments collected from the southernmost portion of the marine cavity beneath RIS. Our record reveals the exposure of subglacial sediments underlying Whillans Ice Stream to marine water ~7 kyr B.P. Combined with the broader record of Ross Sea deglaciation, our work supports a retreat and readvance of the grounding line but amends previously modeled timing from the early-Holocene to the mid-Holocene. Our retreat chronology reveals a variable Siple Coast grounding line during a time of much lower amplitude climate variability than during the last glacial period. This work lends insight into the response of dynamically connected ice streams to physiography, bathymetric controls, and distinct far-field forcing. Furthermore, our data demonstrate that RPO ^{14}C dating improves upon the inherent ambiguity of bulk radiocarbon dating in subglacial sediments and can be used to constrain retreat chronology using sub-ice AIOM.

Data Availability Statement

The complete data set for this manuscript is included in Tables 1, S1, and S2. All geochemical results for this study are publicly available online (at www.doi.org/10.15784/601360).

Acknowledgments

This work was supported by the U.S. National Science Foundation, Section for Antarctic Sciences, Antarctic Integrated System Science program as part of two subglacial access projects: Whillans Ice Stream Subglacial Access Research Drilling (WISSARD; NSF Grants OPP-0839059, OPP-0839142, OPP-0838933, and OPP-0838885) and Subglacial Antarctic Lakes Scientific Access (SALSA; NSF Grants OPP-1543347, OPP-1543537, and OPP-1543441). We thank the University of Nebraska, Lincoln, drill team for borehole access that enabled sample collection, the WISSARD Science Team (see wissard.org for a list of members) for their work in the field, Raytheon Polar Services and Antarctic Support Contract (ASC) for logistical support, and the New York Air National Guard and Ken Borek Air for air support in the field. We acknowledge R. Scherer, R. Powell, and S. Tulaczyk for collection of the WGZ sediment core used in this study. We thank the GMT team for their continued support of the software package; Figure 1 was produced using GMT6/pyGMT (Wessel et al., 2019). This paper benefitted from discussions with C. Schafer, A. Michaud, C. Gustafson, and M. Patterson as well as insightful criticisms and feedback from L. Simkins and one anonymous reviewer.

References

Alley, R. B. (1989). Water-pressure coupling of sliding and bed deformation: I. Water system. *Journal of Glaciology*, *35*(119), 108–118. https://doi.org/10.3189/002214389793701527

Alley, R. B., Anandakrishnan, S., Dupont, T. K., Parizek, B. R., & Pollard, D. (2007). Effect of sedimentation on ice-sheet grounding-line stability. *Science*, *315*(5820), 1838–1841. https://doi.org/10.1126/science.1138396

Alley, R. B., Blankenship, D. D., Bentley, C. R., & Rooney, S. T. (1986). Deformation of till beneath ice stream B, West Antarctica. *Nature*, *322*(6074), 57–59. https://doi.org/10.1038/322057a0

Anandakrishnan, S., Catania, G. A., Alley, R. B., & Horgan, H. J. (2007). Discovery of till deposition at the grounding line of Whillans Ice Stream. *Science*, *315*(5820), 1835–1838. https://doi.org/10.1126/science.1138393

Anderson, J. B., Conway, H., Bart, P. J., Witus, A. E., Greenwood, S. L., McKay, R. M., et al. (2014). Ross Sea paleo-ice sheet drainage and deglacial history during and since the LGM. *Quaternary Science Reviews*, *100*, 31–54. https://doi.org/10.1016/j.quascirev.2013.08.020

Anderson, J. B., Shipp, S. S., Lowe, A. L., Wellner, J. S., & Mosola, A. B. (2002). The Antarctic Ice Sheet during the Last Glacial Maximum and its subsequent retreat history: A review. *Quaternary Science Reviews*, *21*(1–3), 49–70. https://doi.org/10.1016/s0277-3791(01)00083-x

Bao, R., McNichol, A. P., Hemingway, J. D., Gaylord, M. C. L., & Eglinton, T. I. (2019). Influence of different acid treatments on the radiocarbon content spectrum of sedimentary organic matter determined by RPO/Accelerator Mass Spectrometry. *Radiocarbon*, *61*(2), 395–413. https://doi.org/10.1017/rdc.2018.125

Bart, P. J., Anderson, J. B., & Nitsche, F. (2017). Post-LGM grounding-line positions of the Bindschadler paleo ice stream in the Ross Sea Embayment, Antarctica. *Journal of Geophysical Research: Earth Surface*, *122*, 1827–1844. https://doi.org/10.1002/2017JF004259

Bart, P. J., Krogmeier, B. J., Bart, M. P., & Tulaczyk, S. (2017). The paradox of a long grounding during West Antarctic Ice Sheet retreat in Ross Sea. *Scientific Reports*, *7*(1), 1–8. https://doi.org/10.1038/s41598-017-01329-8

Begeman, C. B., Tulaczyk, S., Padman, L., King, M., Siegfried, M. R., Hodson, T. O., & Fricker, H. A. (2020). Tidal pressurization of the ocean cavity near an Antarctic ice shelf grounding line. *Journal of Geophysical Research: Oceans*, *125*, e2019JC015562. https://doi.org/10.1029/2019JC015562

Begeman, C. B., Tulaczyk, S. M., Marsh, O. J., Mikucki, J. A., Stanton, T. P., Hodson, T. O., et al. (2018). Ocean stratification and low melt rates at the Ross Ice Shelf grounding zone. *Journal of Geophysical Research: Oceans*, *123*, 7438–7452. https://doi.org/10.1029/2018JC013987

Bentley, M. J., Cofaigh, C. O., Anderson, J. B., Conway, H., Davies, B., Graham, A. G., et al. (2014). A community-based geological reconstruction of Antarctic Ice Sheet deglaciation since the Last Glacial Maximum. *Quaternary Science Reviews*, *100*, 1–9. https://doi.org/10.1016/j.quascirev.2014.06.025

Blankenship, D. D., Bentley, C. R., Rooney, S. T., & Alley, R. B. (1986). Seismic measurements reveal a saturated porous layer beneath an active Antarctic ice stream. *Nature*, *322*(6074), 54. https://doi.org/10.1038/322054a0

Christianson, K., Jacobel, R. W., Horgan, H. J., Alley, R. B., Anandakrishnan, S., Holland, D. M., & DallaSanta, K. J. (2016). Basal conditions at the grounding zone of Whillans Ice Stream, West Antarctica, from ice-penetrating radar. *Journal of Geophysical Research: Earth Surface*, *121*, 1954–1983. https://doi.org/10.1002/2015JF003806

Christianson, K., Parizek, B. R., Alley, R. B., Horgan, H. J., Jacobel, R. W., Anandakrishnan, S., et al. (2013). Ice sheet grounding zone stabilization due to till compaction. *Geophysical Research Letters*, *40*, 5406–5411. https://doi.org/10.1002/2013gl057447

Christoffersen, P., Tulaczyk, S., & Behar, A. (2010). Basal ice sequences in Antarctic ice stream: Exposure of past hydrologic conditions and a principal mode of sediment transfer. *Journal of Geophysical Research*, *115*, F03034. https://doi.org/10.1029/2009JF001430

Clough, J. W., & Hansen, B. L. (1979). The Ross Ice Shelf Project. *Science*, *203*(4379), 433–434. https://doi.org/10.1126/science.203.4379.433

Coenen, J. J., Scherer, R., Baudoin, P., Warny, S., Castañeda, I. S., & Askin, R. (2019). Paleogene marine and terrestrial development of the West Antarctic Rift System. *Geophysical Research Letters*, *47*. https://doi.org/10.1029/2019GL085281

Conway, H., Hall, B. L., Denton, G. H., Gades, A. M., & Waddington, E. D. (1999). Past and future grounding-line retreat of the West Antarctic Ice Sheet. *Science*, *286*(5438), 280–283. https://doi.org/10.1126/science.286.5438.280

DeConto, R. M., & Pollard, D. (2016). Contribution of Antarctica to past and future sea-level rise. *Nature*, *531*(7596), 591–597. https://doi.org/10.1038/nature17145

Depoorter, M. A., Bamber, J. L., Griggs, J. A., Lenaerts, J. T., Ligtenberg, S. R., van den Broeke, M. R., & Moholdt, G. (2013). Calving fluxes and basal melt rates of Antarctic ice shelves. *Nature*, *502*(7469), 89–92. https://doi.org/10.1038/nature12567

Fernandez, A., Santos, G. M., Williams, E. K., Pendergraft, M. A., Vetter, L., & Rosenheim, B. E. (2014). Blank corrections for ramped pyrolysis radiocarbon dating of sedimentary and soil organic carbon. *Analytical Chemistry*, *86*(24), 12,085–12,092. https://doi.org/10.1021/ac502874j

Golledge, N. R., Kowalewski, D. E., Naish, T. R., Levy, R. H., Fogwill, C. J., & Gasson, E. G. (2015). The multi-millennial Antarctic commitment to future sea-level rise. *Nature*, *526*(7573), 421–425. https://doi.org/10.1038/nature15706

Gomez, N., Mitrovica, J. X., Tamisiea, M. E., & Clark, P. U. (2010). A new projection of sea level change in response to collapse of marine sectors of the Antarctic Ice Sheet. *Geophysical Journal International*, *180*(2), 623–634. https://doi.org/10.1111/j.1365-246x.2009.04419.x

Greenwood, S. L., Simkins, L. M., Halberstadt, A. R. W., Prothro, L. O., & Anderson, J. B. (2018). Holocene reconfiguration and readvance of the East Antarctic Ice Sheet. *Nature Communications*, *9*(1), 1, 3176–12. https://doi.org/10.1038/s41467-018-05625-3

Halberstadt, A. R. W., Simkins, L. M., Greenwood, S. L., & Anderson, J. B. (2016). Past ice-sheet behaviour: Retreat scenarios and changing controls in the Ross Sea, Antarctica. *The Cryosphere*, *10*, 1003–1020. https://doi.org/10.5194/tc-10-1003-2016

Hall, B. L., & Denton, G. H. (2000). Radiocarbon chronology of Ross Sea drift, eastern Taylor Valley, Antarctica: Evidence for a grounded ice sheet in the Ross Sea at the Last Glacial Maximum. *Geografiska Annaler. Series A, Physical Geography*, *82*(2–3), 305–336. https://doi.org/10.1111/1468-0459.00127

Hall, B. L., Denton, G. H., Stone, J. O., & Conway, H. (2013). History of the grounded ice sheet in the Ross Sea sector of Antarctica during the Last Glacial Maximum and the last termination. *Geological Society, London, Special Publications*, *381*(1), 167–181. https://doi.org/10.1144/SP381.5

Hall, B. L., Henderson, G. M., Baroni, C., & Kellogg, T. B. (2010). Constant Holocene Southern-Ocean ^{14}C reservoir ages and ice-shelf flow rates. *Earth and Planetary Science Letters*, *296*(1–2), 115–123. https://doi.org/10.1016/j.epsl.2010.04.054

Harwood, D. M., Scherer, R. P., & Webb, P. N. (1989). Multiple Miocene marine productivity events in West Antarctica as recorded in Upper Miocene sediments beneath the Ross Ice Shelf (Site J-9). *Marine Micropaleontology*, *15*(1–2), 91–115. https://doi.org/10.1016/0377-8398(89)90006-6

Heaton, T.J., Köhler, P., Butzin, M., Bard, E., Reimer, R.W., Austin, W.E.N., et al. (2020). Marine20-the marine radiocarbon age calibration curve (0-55,000 cal BP). *Radiocarbon*, *62*. https://doi.org/10.1017/RDC.2020.68

Hemingway, J. D. (2017). *rampedpyrox: Open-source tools for thermoanalytical data analysis, 2016*. https://doi.org/10.5281/zenodo.839815

Hemingway, J. D., Hilton, R. G., Hovius, N., Eglinton, T. I., Haghipour, N., Wacker, L., et al. (2018). Microbial oxidation of lithospheric organic carbon in rapidly eroding tropical mountain soils. *Science*, *360*(6385), 209–212. https://doi.org/10.1126/science.aao6463

Hemingway, J. D., Rothman, D. H., Rosengard, S. Z., & Galy, V. V. (2017). Technical note: An inverse method to relate organic carbon reactivity to isotope composition from serial oxidation. *Biogeosciences*, *14*(22), 5099–5114. https://doi.org/10.5194/bg-14-5099-2017

Horgan, H. J., Alley, R. B., Christianson, K., Jacobel, R. W., Anandakrishnan, S., Muto, A., et al. (2013). Estuaries beneath ice sheets. *Geology*, *41*(11), 1159–1162. https://doi.org/10.1130/g34654.1

Horgan, H. J., Christianson, K., Jacobel, R. W., Anandakrishnan, S., & Alley, R. B. (2013). Sediment deposition at the modern grounding zone of Whillans Ice Stream, West Antarctica. *Geophysical Research Letters*, *40*, 3934–3939. https://doi.org/10.1002/grl.50712

Horrigan, S. G. (1981). Primary production under the Ross Ice Shelf, Antarctica1. *Limnology and Oceanography*, *26*(2), 378–382. https://doi.org/10.4319/lo.1981.26.2.0378

Hughes, T. (1973). Is the West Antarctic Ice Sheet disintegrating? *Journal of Geophysical Research*, *78*(33), 7884–7910. https://doi.org/10.1029/jc078i033p07884

Jacobel, R. W., Christianson, K., Wood, A. C., Dallasanta, K. J., & Gobel, R. M. (2014). Morphology of basal crevasses at the grounding zone of Whillans Ice Stream, West Antarctica. *Annals of Glaciology*, *55*(67), 57–63. https://doi.org/10.3189/2014aog67a004

Joughin, I., Shean, D. E., Smith, B. E., & Dutrieux, P. (2016). Grounding line variability and subglacial lake drainage on Pine Island Glacier, Antarctica. *Geophysical Research Letters*, *43*, 9093–9102. https://doi.org/10.1002/2016GL070259

Kamb, B. (2001). Basal zone of the West Antarctic ice streams and its role in lubrication of their rapid motion. *The West Antarctic Ice Sheet: behavior and environment*, *77*, 157–199. https://doi.org/10.1029/AR077p0157

King, T. M., Rosenheim, B. E., Post, A. L., Gabris, T., Burt, T., & Domack, E. W. (2018). Large-scale intrusion of circumpolar deep water on Antarctic margin recorded by stylasterid corals. *Paleoceanography and Paleoclimatology*, *33*, 1306–1321. https://doi.org/10.1029/2018PA003439

Kingslake, J., Scherer, R. P., Albrecht, T., Coenen, J., Powell, R. D., Reese, R., et al. (2018). Extensive retreat and re-advance of the West Antarctic Ice Sheet during the Holocene. *Nature*, *558*(7710), 430–434. https://doi.org/10.1038/s41586-018-0208-x

Licht, K. J. (2004). The Ross Sea's contribution to eustatic sea level during meltwater pulse 1A. *Sedimentary Geology*, *165*(3–4), 343–353. https://doi.org/10.1016/j.sedgeo.2003.11.020

Lowry, D. P., Golledge, N. R., Bertler, N. A., Jones, R. S., & McKay, R. (2019). Deglacial grounding-line retreat in the Ross Embayment, Antarctica, controlled by ocean and atmosphere forcing. *Science Advances*, *5*(8), eaav8754. https://doi.org/10.1126/sciadv.aav8754

MacGregor, J. A., Anandakrishnan, S., Catania, G. A., & Winebrenner, D. P. (2011). The grounding zone of the Ross Ice Shelf, West Antarctica, from ice-penetrating radar. *Journal of Glaciology*, *57*(205), 917–928. https://doi.org/10.3189/002214311798043780

Matsuoka, K., Hindmarsh, R. C., Moholdt, G., Bentley, M. J., Pritchard, H. D., Brown, J., et al. (2015). Antarctic ice rises and rumples: Their properties and significance for ice-sheet dynamics and evolution. *Earth-Science Reviews*, *150*, 724–745. https://doi.org/10.1016/j.earscirev.2015.09.004

McKay, R., Golledge, N. R., Maas, S., Naish, T., Levy, R., Dunbar, G., & Kuhn, G. (2016). Antarctic marine ice-sheet retreat in the Ross Sea during the early Holocene. *Geology*, *44*(1), 7–10. https://doi.org/10.1130/g37315.1

Mercer, J. H. (1978). West Antarctic Ice Sheet and CO2 greenhouse effect: A threat of disaster. *Nature*, *271*(5643), 321. https://doi.org/10.1038/271321a0

Morlighem, M. (2019). *MEaSUREs BedMachine Antarctica, Version 1*. Boulder, Colorado USA: NASA National Snow and Ice Data Center Distributed Active Archive Center. https://doi.org/10.5067/C2GFER6PTOS4

Morlighem, M., Rignot, E., Binder, T., Blankenship, D., Drews, R., Eagles, G., et al. (2020). Deep glacial troughs and stabilizing ridges unveiled beneath the margins of the Antarctic ice sheet. *Nature Geoscience*, *13*(2), 132–137. https://doi.org/10.1038/s41561-019-0510-8

Mosola, A. B., & Anderson, J. B. (2006). Expansion and rapid retreat of the West Antarctic Ice Sheet in eastern Ross Sea: Possible consequence of over-extended ice streams? *Quaternary Science Reviews*, *25*(17–18), 2177–2196. https://doi.org/10.1016/j.quascirev.2005.12.013

Mouginot, J., Rignot, E., & Scheuchl, B. (2019). Continent-wide, interferometric SAR phase, mapping of Antarctic ice velocity. *Geophysical Research Letters*, *46*, 9710–9718. https://doi.org/10.1029/2019GL083826

Pendergraft, M. A., & Rosenheim, B. E. (2014). Varying relative degradation rates of oil in different forms and environments revealed by ramped pyrolysis. *Environmental Science & Technology*, *48*(18), 10,966–10,974. https://doi.org/10.1021/es501354c

Priscu, J. C., Downes, M. T., Priscu, L. R., Palmisano, A. C., & Sullivan, C. W. (1990). Dynamics of ammonium oxidizer activity and nitrous oxide (N_2O) within and beneath Antarctic Sea Ice. *Marine Ecology Progress Series*, *62*, 37–46. https://doi.org/10.3354/meps062037

Prothro, L. O., Majewski, W., Yokoyama, Y., Simkins, L. M., Anderson, J. B., Yamane, M., et al. (2020). Timing and pathways of East Antarctic Ice Sheet retreat. *Quaternary Science Reviews*, *230*, 106166. https://doi.org/10.1016/j.quascirev.2020.106166

Rack, F. R. (2016). Enabling clean access into subglacial Lake Whillans: Development and use of the WISSARD hot water drill system. *Philosophical Transactions of the Royal Society A: Mathematical, Physical and Engineering Sciences*, *374*(2059), 20140305. https://doi.org/10.1098/rsta.2014.0305

Rignot, E., & Jacobs, S. S. (2002). Rapid bottom melting widespread near Antarctic ice sheet grounding lines. *Science*, *296*(5575), 2020–2023. https://doi.org/10.1126/science.1070942

Rignot, E., Mouginot, J., Morlighem, M., Seroussi, H., & Scheuchl, B. (2014). Widespread, rapid grounding line retreat of Pine Island, Thwaites, Smith, and Kohler glaciers, West Antarctica, from 1992 to 2011. *Geophysical Research Letters*, *41*, 3502–3509. https://doi.org/10.1002/2014GL060140

Rosenheim, B. E., Day, M. B., Domack, E., Schrum, H., Benthien, A., & Hayes, J. M. (2008). Antarctic sediment chronology by programmed-temperature pyrolysis: Methodology and data treatment. *Geochemistry, Geophysics, Geosystems*, *9*, Q04005. https://doi.org/10.1029/2007GC001816

Rosenheim, B. E., & Galy, V. (2012). Direct measurement of riverine particulate organic carbon age structure. *Geophysical Research Letters*, *39*, L19703. https://doi.org/10.1029/2012GL052883

Rosenheim, B. E., Roe, K. M., Roberts, B. J., Kolker, A. S., Allison, M. A., & Johannesson, K. H. (2013). River discharge influences on particulate organic carbon age structure in the Mississippi/Atchafalaya River System. *Global Biogeochemical Cycles*, *27*, 154–166. https://doi.org/10.1002/gbc.20018

Rosenheim, B. E., Santoro, J. A., Gunter, M., & Domack, E. W. (2013). Improving Antarctic sediment ^{14}C dating using ramped pyrolysis: An example from the Hugo Island Trough. *Radiocarbon*, *55*, 115–126. https://doi.org/10.1017/s0033822200047846

Scambos, T. A., Haran, T. M., Fahnestock, M. A., Painter, T. H., & Bohlander, J. (2007). MODIS-based mosaic of Antarctica (MOA) data sets: Continent-wide surface morphology and snow grain size. *Remote Sensing of Environment*, *111*(2–3), 242–257. https://doi.org/10.1016/j.rse.2006.12.020

Scherer, R. P. (1991). Quaternary and Tertiary microfossils from beneath Ice Stream B: Evidence for a dynamic West Antarctic Ice Sheet history. *Global and Planetary Change*, *4*(4), 395–412. https://doi.org/10.1016/0921-8181(91)90005-h

Scherer, R. P. (1994). A new method for the determination of absolute abundance of diatoms and other silt-sized sedimentary particles. *Journal of Paleolimnology*, *12*(2), 171–179. https://doi.org/10.1007/bf00678093

Scherer, R. P., Aldahan, A., Tulaczyk, S., Possnert, G., Engelhardt, H., & Kamb, B. (1998). Pleistocene collapse of the West Antarctic Ice Sheet. *Science*, *281*(5373), 82–85. https://doi.org/10.1126/science.281.5373.82

Schoof, C. (2007). Ice sheet grounding line dynamics: Steady states, stability, and hysteresis. *Journal of Geophysical Research*, *112*, F03S28. https://doi.org/10.1029/2006JF000664

Schreiner, K. M., Bianchi, T. S., & Rosenheim, B. E. (2014). Evidence for permafrost thaw and transport from an Alaskan North Slope watershed. *Geophysical Research Letters*, *41*, 3117–3126. https://doi.org/10.1002/2014GL059514

Siegfried, M. R., & Fricker, H. A. (2018). Thirteen years of subglacial lake activity in Antarctica from multi-mission satellite altimetry. *Annals of Glaciology*, *59*(76pt1), 42–55. https://doi.org/10.1017/aog.2017.36

Simkins, L. M., Greenwood, S. L., & Anderson, J. B. (2018). Diagnosing ice sheet grounding line stability from landform morphology. *The Cryosphere*, *12*, 2707–2726. https://doi.org/10.5194/tc-12-2707-2018

Smith, J. A., Graham, A. G., Post, A. L., Hillenbrand, C. D., Bart, P. J., & Powell, R. D. (2019). The marine geological imprint of Antarctic ice shelves. *Nature Communications*, *10*(1), 1, 5635–16. https://doi.org/10.1038/s41467-019-13496-5

Spector, P., Stone, J., Cowdery, S. G., Hall, B., Conway, H., & Bromley, G. (2017). Rapid early-Holocene deglaciation in the Ross Sea, Antarctica. *Geophysical Research Letters*, *44*, 7817–7825. https://doi.org/10.1002/2017GL074216

Stuiver, M., Denton, G. H., Hughes, T. J., & Fastook, J. L. (1981). History of the marine ice sheets in West Antarctica during the last glaciation: A working hypothesis. In G. H. Denton, & T. J. Hughes (Eds.), *The Last Great Ice Sheets* (pp. 319–439). New York: Wiley-Interscience.

Stuiver, M., & Polach, H. A. (1977). Discussion reporting of ^{14}C data. *Radiocarbon*, *19*(3), 355–363. https://doi.org/10.1017/s0033822200003672

Subt, C., Fangman, K. A., Wellner, J. S., & Rosenheim, B. E. (2016). Sediment chronology in Antarctic deglacial sediments: Reconciling organic carbon ^{14}C ages to carbonate ^{14}C ages using Ramped PyrOx. *The Holocene*, *26*(2), 265–273. https://doi.org/10.1177/0959683615608688

Subt, C., Yoon, H. I., Yoo, K. C., Lee, J. I., Leventer, A., Domack, E. W., & Rosenheim, B. E. (2017). Sub-ice shelf sediment geochronology utilizing novel radiocarbon methodology for highly detrital sediments. *Geochemistry, Geophysics, Geosystems*, *18*, 1404–1418. https://doi.org/10.1002/2016gc006578

Tinto, K. J., Padman, L., Siddoway, C. S., Springer, S. R., Fricker, H. A., Das, I., et al. (2019). Ross Ice Shelf response to climate driven by the tectonic imprint on seafloor bathymetry. *Nature Geoscience*, *12*(6), 441–449. https://doi.org/10.1038/s41561-019-0370-2

Tulaczyk, S., Mikucki, J. A., Siegfried, M. R., Priscu, J. C., Barcheck, C. G., Beem, L. H., et al. (2014). WISSARD at subglacial Lake Whillans, West Antarctica: Scientific operations and initial observations. *Annals of Glaciology*, *55*(65), 51–58. https://doi.org/10.3189/2014aog65a009

Vick-Majors, T. J., Michaud, A. B., Skidmore, M. L., Turetta, C., Barbante, C., Christner, B. C., et al. (2020). Biogeochemical connectivity between freshwater ecosystems beneath the West Antarctic Ice Sheet and the sub-ice marine environment. *Global Biogeochemical Cycles*, *34*, e2019GB006446. https://doi.org/10.1029/2019GB006446

Villinski, J. C., Dunbar, R. B., & Mucciarone, D. A. (2000). Carbon 13/Carbon 12 ratios of sedimentary organic matter from the Ross Sea, Antarctica: A record of phytoplankton bloom dynamics. *Journal of Geophysical Research*, *105*(C6), 14,163–14,172. https://doi.org/10.1029/1999JC000309

Warnock, J. P., & Scherer, R. P. (2015). A revised method for determining the absolute abundance of diatoms. *Journal of Paleolimnology*, *53*(1), 157–163. https://doi.org/10.1007/s10933-014-9808-0

Weertman, J. (1974). Stability of the junction of an ice sheet and an ice shelf. *Journal of Glaciology*, *13*(67), 3–11. https://doi.org/10.3189/s0022143000023327

Wessel, P., Luis, J. F., Uieda, L., Scharroo, R., Wobbe, F., Smith, W. H. F., & Tian, D. (2019). The Generic Mapping Tools Version 6. *Geochemistry, Geophysics, Geosystems*, *20*, 5556–5564. https://doi.org/10.1029/2019GC008515

Whitehouse, P. L., Gomez, N., King, M. A., & Wiens, D. A. (2019). Solid Earth change and the evolution of the Antarctic Ice Sheet. *Nature Communications*, *10*(1), 1, 503–14. https://doi.org/10.1038/s41467-018-08068-y

Williams, E. K., Rosenheim, B. E., Allison, M., McNichol, A. P., & Xu, L. (2015). Quantification of refractory organic material in Amazon mudbanks of the French Guiana Coast. *Marine Geology*, *363*, 93–101. https://doi.org/10.1016/j.margeo.2015.02.009

Zhang, X., Bianchi, T. S., Cui, X., Rosenheim, B. E., Ping, C. L., Hanna, A. J., et al. (2017). Permafrost organic carbon mobilization from the watershed to the Colville River Delta: Evidence from ^{14}C ramped pyrolysis and lignin biomarkers. *Geophysical Research Letters*, *44*, 11,491–11,500. https://doi.org/10.1002/2017GL075543

Erratum

In the originally published version of this article, there was an error in calibrating the data. This error has been corrected and the change resulting in the processing error yields a noticeable change in calibrated ages, but does not alter the main conclusions of the published manuscript. The file and Figure 3b have been updated, and the present version may be considered the authoritative version of record.